Temperature-dependent recombination coefficients in InGaN light-emitting diodes: Hole localization, Auger processes, and the green gap

Felix Nippert,[1] Sergey Yu. Karpov,[2] Gordon Callsen,[1] Bastian Galler,[3] Thomas Kure,[1] Christian Nenstiel,[1] Markus R. Wagner,[1] Martin Straßburg,[3] Hans-Jürgen Lugauer,[3] and Axel Hoffmann[1]
[1]*Institut für Festkörperphysik, Technische Universität Berlin, Hardenbergstraße 36, 10623 Berlin, Germany*
[2]*STR Group–Soft-Impact Ltd., P.O. Box 83, 27 Engels av., 194156 St. Petersburg, Russia*
[3]*OSRAM Opto Semiconductors GmbH, Leibnizstraße 4, 93055 Regensburg, Germany*

(Received 2 August 2016; accepted 6 October 2016; published online 18 October 2016)

We obtain temperature-dependent recombination coefficients by measuring the quantum efficiency and differential carrier lifetimes in the state-of-the-art InGaN light-emitting diodes. This allows us to gain insight into the physical processes limiting the quantum efficiency of such devices. In the green spectral range, the efficiency deteriorates, which we assign to a combination of diminishing electron-hole wave function overlap and enhanced Auger processes, while a significant reduction in material quality with increased In content can be precluded. Here, we analyze and quantify the entire balance of all loss mechanisms and highlight the particular role of hole localization. *Published by AIP Publishing*. [http://dx.doi.org/10.1063/1.4965298]

Light-emitting diodes (LEDs) with InGaN/GaN multi quantum well (MQW) active regions are widely used as visible light emitters for solid-state lighting. However, such LEDs still suffer considerably from two phenomena: the so-called "green gap," that is, LED efficiency reduction in the green/yellow spectral range,[1,2] and efficiency droop[2–4] observed at high operating currents. The physical nature of the green gap is still debated extensively.[5,6] In order to shift the emission wavelength to the green/yellow spectral region, it is necessary to increase the In content in InGaN QWs. This may lead to stress relaxation via dislocation formation in the QWs, as a prominent lattice-mismatch with the surrounding GaN layers arises.[7] In addition, higher In content is normally achieved by lowering the InGaN growth temperature,[8] which favors point defect formation.[9] Both, extended and point defects should promote Shockley-Read-Hall (SRH) recombination,[10] thus reducing LED efficiency. Further, increased In content also gives rise to the quantum-confined Stark effect (QCSE),[11,12] which reduces the electron-hole wave function overlap, and hence the rate of radiative recombination.[13,14] Unfortunately, none of the above mentioned effects can explain quantitatively the magnitude of the reduction of LED efficiency,[15] still observed even in devices of the highest quality.[16] For a long time, explanations for the efficiency droop were also controversial.[4] Hotly debated, the droop phenomenon has been assigned experimentally to (phonon-assisted) Auger recombination.[17–19] Deeper insight into the mechanisms critical for both, the green gap and the efficiency droop, may be achieved by measuring the recombination coefficients (RCs). Previous studies have considered room temperature RCs as a function of emission wavelength,[10,20] or temperatures above room temperature.[21] Determination of the RCs over a larger temperature range permits to decouple temperature-independent factors, such as QCSE, from temperature dependent ones, for example, carrier localization. In this Letter, we report on SRH, radiative and Auger RCs, measured in a wide temperature range for state-of-the-art blue- and green-emitting InGaN MQW LEDs. Our findings exclude inferior InGaN material quality from the list of potential causes for the green gap. In addition, we unravel and quantify the contributions of decreasing electron-hole wave function overlap and enhanced Auger recombination. Finally, we consider the increasing hole localization in InGaN alloys with higher indium composition in order to explain the temperature dependences of the RCs. For our study, MQW LEDs were grown by metal-organic vapor phase epitaxy on c-plane sapphire substrates. The devices emit at a wavelength of 445 nm (530 nm) and contain five (seven) QWs. The InGaN QWs were embedded in GaN barriers, comprising Si-doped n-GaN layers below the active region, and Mg-doped p-GaN, and AlGaN electron blocking layers on the top. The devices were packaged in OSRAM's commercial Golden Dragon+ package and represent the state-of-the-art epitaxial quality. Our method for an evaluation of the RCs is based on the ABC-model[22–24] considering the dependence of the LED external quantum efficiency (EQE) on the carrier concentration in the active region n in the form: $\mathrm{EQE} = \eta_{ext} Bn/(A + Bn + Cn^2)$. Here, η_{ext} is the light extraction efficiency, while the RCs A, B and C correspond to SRH, radiative, and Auger recombination, respectively. The method implies simultaneous measurements of the EQE and the differential carrier lifetime (DLT) by small-signal time-resolved photoluminescence (SSTRPL) *versus* LED operating current.[25] The EQE of our LEDs as a function of operating current was measured by integrating pulsed electroluminescence (EL), a standard method.[26] The EL spectra were recorded with a Princeton Instruments charge-coupled device through a 30 cm focal length SpectraPro monochromator. By evaluating the EQE as a function of normalized optical output power p (i.e., $p = 1$ at the maximum value of EQE – EQE_{max}), the so-called quality factor $Q = B/(AC)^{1/2}$ can be found via the relationship[26]

$$\frac{\mathrm{EQE}_{max}}{\mathrm{EQE}} = \frac{Q + p^{1/2} + p^{-1/2}}{Q + 2}. \quad (1)$$

For the DLT measurements, the LEDs were pumped electrically with a DC current and in addition optically with a frequency-doubled Ti:Sa laser tuned to 400 nm, guaranteeing optical absorption in the InGaN QWs exclusively. Details regarding the measurement procedure, data evaluation, and a discussion about the necessity of optical pumping for DLT measurements in InGaN structures can be found in Ref. 25. From the measured DLT (τ), the SRH RC A can be found based on the following equation:

$$\tau = \frac{A^{-1}}{1 + 2Qp^{1/2} + 3p}. \tag{2}$$

Further evaluation of the sheet radiative $[B_{2D} = A^2Q(2+Q)(qS/I_{max})]$ and sheet Auger $[C_{2D} = A^3(2+Q)^2(qS/I_{max})^2)]$ RCs is straightforward.[25] Here, I_{max} is the current corresponding to the EQE maximum, S is the active region area, and q is the elementary charge. Note that both, A and Q, are independent of I_{max}; moreover, the Q-factor does not depend on whether bulk RCs B and C or sheet RCs B_{2D} and C_{2D} are used for its determination. As soon as the Q-factor is known, the maximum IQE value $IQE_{max} = Q/(Q+2)$ can be easily estimated. Figure 1(a) shows the IQE of typical blue and green MQW LEDs as a function of normalized optical output power p. While the EQE datasets are measured in arbitrary units, their fitting by Eq. (1) allows the determination of the quality factor Q, and hence, the dependence of IQE on p in absolute units (solid lines in Fig. 1(a)). We wish to remark, that at low temperatures (<150 K) and low currents ($p < 1$), the behavior of green LEDs is found to deviate from the ABC model: The measured IQE is higher than predicted by theory. This implies that in this regime, the RCs are not independent of the injection level anymore, and the assumptions made to evaluate the RCs do not hold. Therefore, the presented study is confined to the temperature range where the LED efficiency can be well approximated by the ABC-model with constant RCs.[26] This also means that all DLT measurements are performed at $p > 1$—a condition always fulfilled under real world operating conditions. Figure 1(b) displays exemplary SSTRPL traces obtained at 300 K at various currents. The transient decays are mono-exponential and the constant (EL) background has been subtracted for clarity. One can see that the DLTs decrease with rising LED drive current, and thus, with increasing carrier density in the active region. Using Eq. (2), these DLTs along with the Q-factors can be used to extract the SRH coefficient A. This is demonstrated in Fig. 1(c) for blue and green MQW LEDs at a temperature of 300 K. Here the measured DLT trends (circles) are approximated with Eq. (2) (solid lines) for unambiguous values of the A. Figure 2 summarizes the main results of our extended study. Filled blue squares (green diamonds) in Fig. 2 correspond to blue (green) MQW LEDs. The IQE of green-emitting devices is found to be much lower than that of blue-emitting ones, cf. Fig. 1(a), indicating the green gap behavior. Further, it can be observed that the efficiency of the green LEDs is lower than that of blue ones even at low temperatures and exhibits a more pronounced decline with temperature. Usually, the green gap is explained by a rise in the point/structural defect density in the InGaN QWs with high In content—an enhanced SRH recombination—or by a decreased overlap between electron and hole wave functions due to the QCSE, lowering the radiative recombination. Naturally, also a combination of both factors seems plausible at first glance. In contrast, we have obtained almost identical SRH RCs A for our blue (445 nm) and green (530 nm) LEDs over the whole temperature range (see Fig. 2(a)). Consequently, very similar SRH-related activation energies E_A of 54 meV and 52 meV can be obtained. A similar result has been reported earlier for room temperature only.[10,16] In our case, the identical temperature dependence of the SRH RC over a wide temperature range provides strong evidence for a well-comparable crystal quality of the InGaN QWs for blue and green light emission, which is attained despite the very different compositions of the InGaN alloys. This means, that the observed IQE reduction towards longer emission wavelength cannot be associated with an assumed enhanced defect generation at higher

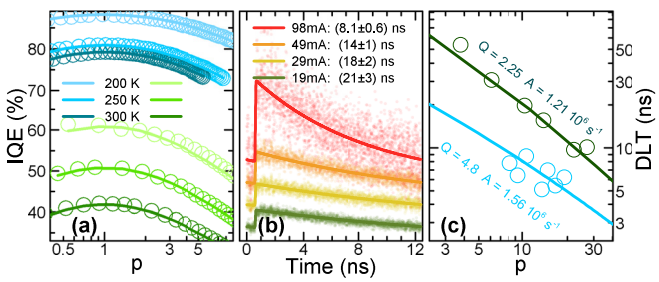

FIG. 1. (a) IQE as a function of p for a blue and a green MQW LEDs at different T. Circles correspond to data points, while solid lines are fits based on the ABC-model. (b) SSTRPL traces for one of the green devices at $T = 300$ K at various currents. Circles correspond to data points and solid lines show mono-exponential fits (see Ref. 25 for details). (c) Exemplary evaluation of the SRH-RC A. Blue (green) points are measured DLTs of a blue (green) MQW LED at $T = 300$ K. Solid lines depict fits to the data based on Eq. (2).

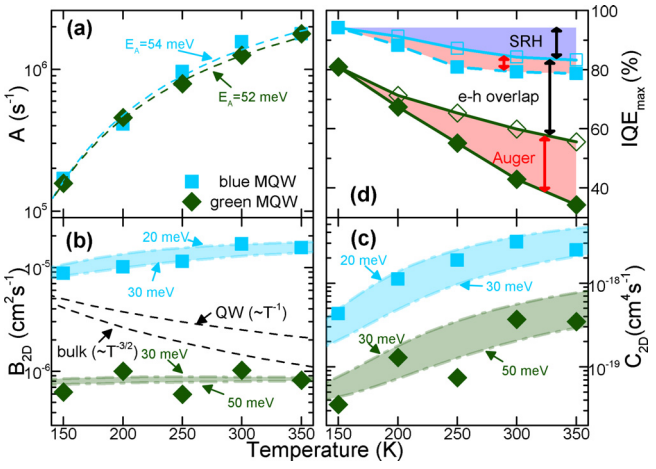

FIG. 2. Temperature dependence of the RCs corresponding to (a) SRH, (b) radiative, and (c) Auger recombination. Blue squares (green diamonds) refer to blue-emitting (green-emitting) MQW LEDs. The blue (green) shaded areas show theoretical estimates made for certain ranges of the hole localization energy (see text). (d) Temperature dependence of IQE. Open symbols represent values derived under the assumption that B_{2D} and C_{2D} would not vary with temperature above 150 K. The shaded areas demonstrate the impact of several mechanisms to IQE reduction (see text). Dashed lines in panel (a) and (b) show fits of the activation energy E_A of SRH recombination, and the expected temperature dependence of B in bulk and QW material, respectively.

In content in the QW active region. The radiative (B_{2D}) and Auger (C_{2D}) RCs are shown in Figs. 2(b) and 2(c). Both coefficients are reduced significantly for the green-emitting devices, compared to blue-emitting ones. Whereas recalculation of the sheet RCs to the bulk ones is questionable because of uncertainty in the number of QWs participating effectively in recombination,[25] the observed big difference in both RCs still suggests a substantial reduction in the overlap of electron and hole wave functions in green LEDs. This reduction cannot be, however, attributed entirely to the QCSE arising in the InGaN QWs due to polarization charges at the QW interfaces, which are enhanced with rising In content in the InGaN alloy. Indeed, both, B_{2D} and C_{2D}, are found to increase generally with T (see Figs. 2(b) and 2(c)). While the rise of the Auger RCs with T does not conflict qualitatively with available models considering phonon-assisted processes,[27] a corresponding rise of the radiative RCs (blue LED) or an almost constant behaviour (green LED) is anomalous, as either a proportionality to $T^{-3/2}$ (bulk materials),[28,29] to T^{-1} (QWs),[30,31] or no temperature dependence (quantum dots)[32] is expected in semiconductors (compare with dashed lines in Fig. 2(b)). It should be noted that some traces of a synchronous variation of B and C with T, were previously reported,[26,33] but attributing the anomaly just to the B coefficient has become possible only due to the direct determination of an independent set of the RCs in this study. In order to interpret the observed anomalous temperature dependence of B_{2D}, we consider that a few neighboring In atoms may provide effective carrier localization in InGaN.[6,34,35] Here, a simple model is used, assuming electrons to be completely delocalized and holes to be localized in the bulk of an InGaN alloy due to larger effective masses. The hole localization is characterized by the localization energy E_L counted from the top of the valence band, and the wave function localization radius $a_L = \hbar/(2m_hE_L)^{1/2}$ where $\hbar$ is the reduced Planck constant and m_h is the hole effective mass. Assuming the localized hole wave function to be hydrogen-like, one can calculate the radiative recombination constant[36]

$$B = 64\pi\nu_B\langle a_{eff}\rangle^3, \quad \nu_B = \frac{2\alpha n_r E_g E_P}{3\hbar m_0 c^2}. \tag{3}$$

Here, $\alpha \approx 1/137$ is the fine-structure constant, n_r and E_g are the group refractive index and energy gap of the material, respectively, $E_P = 2m_0P^2/\hbar^2$ is the energy related to Kane's matrix element P,[37] m_0 is the electron mass, and c is the velocity of light in vacuum. The effective localization radius $\langle a_{eff}\rangle$ in Eq. (3) is defined by the expression $\langle a_{eff}\rangle^3 = \rho^{-1}\int_0^\infty g(E_L)f(E_L)a_L^3(E_L)\xi^4(E_L)dE_L$ where $g(E_L)$ is the density of states (DOS) of localized holes, $f(E_L) = [1+\exp[(F_p - E_L)/kT]]^{-1}$ is the Fermi-Dirac distribution function of holes, $\xi(E_L) = m_hE_L/(m_hE_L + m_eE_e)$, m_e is the electron effective mass, and E_e is the mean kinetic energy of delocalized electrons, which is equal to kT in the case of non-degenerate carriers. Additionally, F_p is the quasi-Fermi level for holes, k is the Boltzmann constant, and the concentration of localized holes ρ is defined as: $\rho = \int_0^\infty g(E_L)f(E_L)dE_L$. As follows from Eq. (3), the temperature dependence of the radiative recombination constant B is mainly determined by that of the effective localization radius $\langle a_{eff}\rangle$. For simplicity, assuming the DOS of localized holes to have an exponential form,[38] $g(E) = [1+\exp(E/E_t)]^{-1}$, with E_t being the specific energy of the DOS tail in the energy gap, and using typical values of $n_r = 2.9$, $E_g = 2.7$ eV, $E_P = 14$ eV, $m_e/m_h = 0.1$, $m_h = 2.0m_0$, one can obtain the temperature dependence of the effective localization radius $\langle a_{eff}\rangle$ shown in Fig. 3. Here, one can see that the variation of $\langle a_{eff}\rangle$ (and hence B) with temperature depends remarkably on the localization strength characterized by the parameter E_t and the electron kinetic energy E_e. For non-degenerate electrons (Fig. 3(b)), $\langle a_{eff}\rangle$ increases monotonically, while the slope decreases with rising localization. If higher kinetic energies E_e are assumed (see Fig. 3(a)), the overall, corresponding slope is reduced. With $E_e = 300$ meV, the effective localization radius is even found to increase at low temperatures, followed by a decrease towards higher temperatures ($E_t = 20$ meV) or to be practically independent of temperature ($E_t = 60$ meV). Generally, high-energy electrons possess a reduced overlap with the hole wave functions expressed by the factor ξ, thus causing a reduction of $\langle a_{eff}\rangle$, and consequently, the radiative RC B. We note that in addition to the radiative RC B, where (temperature-independent) calculations have shown a reduction due to random alloying,[6] also the Auger RC C should scale with the electron-hole wave function overlap. The Augur RC C, corresponding to the process involving two delocalized electrons and a localized hole – in line with the experimentally identified dominant Auger process[19,39,40]— can be estimated as[41]

$$C = \frac{(16\pi\sqrt{2})}{3}\langle a_L a_G\rangle^3 \frac{E_D}{\hbar}\frac{E_e}{E_g}, \tag{4}$$

where $a_G = \hbar/\sqrt{2m_e(E_g - E_L)}$ and $\langle a_L a_G\rangle^3 = \rho^{-1}\int_0^\infty g(E_L)f(E_L)a_L^3(E_L)a_G^3(E_L)dE_L$. The shaded areas in Fig. 2(b) show the thermal evolution of the coefficient B calculated by Eq. (3). Here, good agreement can be reached with E_t in the range of 20–30 meV for blue and of 30–50 meV for green LEDs, values well comparable with the literature.[6,34] In order to achieve this direct comparison with the experimental sheet RC, the calculated B values were scaled with constant factors, to account for the uncertainty in the recombination volume and any additional electron-hole-overlap reduction caused by the QCSE. Here, Fig. 2(b) shows a good correlation of the theoretical temperature dependence with the data on the coefficients B_{2D}, directly suggesting stronger hole localization in green LEDs than in the blue ones—as

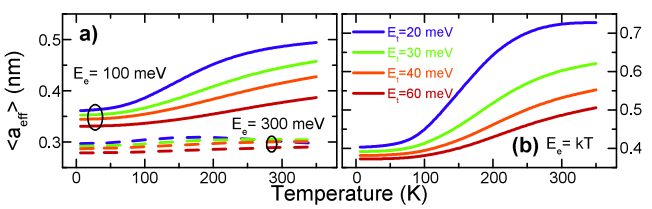

FIG. 3. Temperature dependence of the effective localization radius $\langle a_{eff}\rangle$ calculated for different energies E_t (characteristic for the localization strength) of the hole density of states tail. (a) For constant kinetic energies of electrons E_e, (b) for non-degenerate electrons ($E_e = kT$). A hole Fermi level of $F_p = 100$ meV is assumed for all calculations.

commonly expected.[6] Note that at even higher temperatures, once all holes are delocalized, the B coefficient reduces again.[21] Similarly, temperature-dependent C coefficients calculated for blue and green LEDs by Eq. (4) are presented by the shaded areas in Fig. 2(c) and also correlate with experimental data. The increase of Auger recombination with rising T is more significant than previously predicted in a much narrower temperature range.[27] Naturally not all possible Auger processes are considered in our model, motivating future examinations with focus on phonon-assisted processes. Nevertheless the steep rise of C can already be sufficiently explained by means of hole localization in our simplified model. Based on the determined RCs, we can distinguish between various factors contributing to the green gap. In addition to the observed IQEs (filled symbols), Fig. 2(d) also shows hypothetical IQEs, assuming that their temperature-dependence is determined by the rise in SRH recombination only (open symbols) yielding, for example, $Q(T) = B(150\,\mathrm{K})/\sqrt{A(T)C(150\,\mathrm{K})}$. Consequently, the violet-shaded area indicates the IQE reduction due to SRH recombination that rises with T (150–350 K). The mostly temperature-independent difference between the hypothetical IQE trends for blue and green LEDs (marked by an arrow in Fig. 2(d)) is associated with the different magnitudes of the B and C RCs, and therefore, originates from the decreasing electron-hole-overlap towards the green spectral range, compared to blue LEDs, due to the QCSE and hole localization, as discussed above. The overlap decrease is responsible for about half of the total green gap IQE reduction towards operating temperature (350 K). The red-shaded areas in Fig. 2(d) mark the additional IQE losses due to the specific temperature dependence of the B and C coefficients. As the temperature dependence of B is minor, cf. Fig. 2(b), Auger recombination is the major contributor to such kind of losses. We have found the efficiency losses to be much more pronounced for green LEDs, meaning that the contribution of Auger recombination to the green gap is most significant. The difference between the Auger losses in blue and green LEDs suggests that the more pronounced thermal activation of Auger processes directly correlates with the stronger localization occurring in green InGaN alloys. Naturally, any rise in charge carrier localization enhances the electron-phonon-coupling[42–45] favoring phonon-assisted Auger processes and their impact on the IQE reduction. In conclusion, we have observed close to identical SRH RCs over the entire temperature range for blue- and green-emitting MQW, ruling out defect generation in InGaN with high In content as principal cause of the green gap. In contrast, the radiative and Auger RCs were found to decrease significantly in green-emitting LEDs, because of a reduced overlap between electron and hole wave functions. The anomalous temperature dependence of the radiative recombination allows us to attribute a part of this reduction to hole localization induced by fluctuations of the InGaN composition, while the temperature independent reduction stems from the QCSE. Here, even a simplified model for all recombination processes, involving delocalized electrons and localized holes, suffices to interpret the data. In addition, the strong rise with temperature of the Auger RC leads to a further reduction of quantum efficiency with temperature. This is especially true for green-emitting LEDs, where holes are still substantially localized at operating temperatures.

We acknowledge the financial support from the European Union FP7-ICT Project No. NEWLED (FP7-318388), and the German Science Foundation (CRC 787).

[1]S. Nakamura, M. Senoh, N. Iwasa, and S. Nagahama, Jpn. J. Appl. Phys., Part 2 **34**, L797 (1995).
[2]M. R. Krames, O. B. Shchekin, R. Mueller-Mach, G. O. Mueller, L. Zhou, G. Harbers, and M. G. Craford, J. Disp. Technol. **3**, 160 (2007).
[3]A. Laubsch, M. Sabathil, W. Bergbauer, M. Strassburg, H. Lugauer, M. Peter, S. Lutgen, N. Linder, K. Streubel, J. Hader, J. V. Moloney, B. Pasenow, and S. W. Koch, Phys. Status Solidi C **6**, S913 (2009).
[4]J. Piprek, Phys. Status Solidi A **207**, 2217 (2010).
[5]Y. Jiang, Y. Li, Y. Li, Z. Deng, T. Lu, Z. Ma, P. Zuo, L. Dai, L. Wang, H. Jia, W. Wang, J. Zhou, W. Liu, and H. Chen, Sci. Rep. **5**, 10883 (2015).
[6]M. Auf der Maur, A. Pecchia, G. Penazzi, W. Rodrigues, and A. Di Carlo, Phys. Rev. Lett. **116**, 027401 (2016).
[7]A. Lobanova, A. Kolesnikova, A. Romanov, S. Y. Karpov, M. Rudinsky, and E. Yakovlev, Appl. Phys. Lett. **103**, 152106 (2013).
[8]S. Keller, B. P. Keller, D. Kapolnek, A. C. Abare, H. Masui, L. A. Coldren, U. K. Mishra, and S. P. Den Baars, Appl. Phys. Lett. **68**, 3147 (1996).
[9]S. Hammersley, M. J. Kappers, F. C.-P. Massabuau, S.-L. Sahonta, P. Dawson, R. A. Oliver, and C. J. Humphreys, Appl. Phys. Lett. **107**, 132106 (2015).
[10]D. Schiavon, M. Binder, M. Peter, B. Galler, P. Drechsel, and F. Scholz, Phys. Status Solidi B **250**, 283 (2013).
[11]T. Takeuchi, S. Sota, M. Katsuragawa, M. Komori, H. Takeuchi, H. Amano, and I. Akasaki, Jpn. J. Appl. Phys., Part 2 **36**, L382 (1997).
[12]J. Bai, T. Wang, and S. Sakai, J. Appl. Phys. **88**, 4729 (2000).
[13]J. S. Im, H. Kollmer, J. Off, A. Sohmer, F. Scholz, and A. Hangleiter, Phys. Rev. B **57**, 9435 (1998).
[14]F. Della Sala, A. Di Carlo, P. Lugli, F. Bernardini, V. Fiorentini, R. Scholz, and J.-M. Jancu, Appl. Phys. Lett. **74**, 2002 (1999).
[15]K. Bulashevich, O. Khokhlev, I. Y. Evstratov, and S. Y. Karpov, in Proc. SPIE **8278**, 827819 (2012).
[16]S. Saito, R. Hashimoto, J. Hwang, and S. Nunoue, Appl. Phys. Express **6**, 111004 (2013).
[17]J. Iveland, L. Martinelli, J. Peretti, J. S. Speck, and C. Weisbuch, Phys. Rev. Lett. **110**, 177406 (2013).
[18]M. Binder, A. Nirschl, R. Zeisel, T. Hager, H.-J. Lugauer, M. Sabathil, D. Bougeard, J. Wagner, and B. Galler, Appl. Phys. Lett. **103**, 071108 (2013).
[19]B. Galler, H.-J. Lugauer, M. Binder, R. Hollweck, Y. Folwill, A. Nirschl, A. Gomez-Iglesias, B. Hahn, J. Wagner, and M. Sabathil, Appl. Phys. Express **6**, 112101 (2013).
[20]A. David and M. J. Grundmann, Appl. Phys. Lett. **97**, 033501 (2010).
[21]B. Galler, P. Drechsel, R. Monnard, P. Rode, P. Stauss, S. Froehlich, W. Bergbauer, M. Binder, M. Sabathil, B. Hahn, and J. Wagner, Appl. Phys. Lett. **101**, 131111 (2012).
[22]H.-Y. Ryu, H.-S. Kim, and J.-I. Shim, Appl. Phys. Lett. **95**, 081114 (2009).
[23]Q. Dai, Q. Shan, J. Wang, S. Chhajed, J. Cho, E. F. Schubert, M. H. Crawford, D. D. Koleske, M.-H. Kim, and Y. Park, Appl. Phys. Lett. **97**, 133507 (2010).
[24]S. Karpov, Opt. Quantum Electron. **47**, 1293 (2015).
[25]F. Nippert, S. Karpov, I. Pietzonka, B. Galler, A. Wilm, T. Kure, C. Nenstiel, G. Callsen, M. Straßburg, H.-J. Lugauer, and A. Hoffmann, Jpn. J. Appl. Phys., Part 1 **55**, 05FJ01 (2016).
[26]I. Titkov, S. Karpov, A. Yadav, V. Zerova, M. Zulonas, B. Galler, M. Strassburg, I. Pietzonka, H.-J. Lugauer, and E. Rafailov, IEEE J. Quantum Electron. **50**, 911 (2014).
[27]E. Kioupakis, Q. Yan, D. Steiauf, and C. G. Van de Walle, New J. Phys. **15**, 125006 (2013).
[28]G. Lasher and F. Stern, Phys. Rev. **133**, A553 (1964).
[29]G. W. t Hooft and C. van Opdorp, Appl. Phys. Lett. **42**, 813 (1983).
[30]Y. Arakawa, H. Sakaki, M. Nishioka, J. Yoshino, and T. Kamiya, Appl. Phys. Lett. **46**, 519 (1985).
[31]T. Matsusue and H. Sakaki, Appl. Phys. Lett. **50**, 1429 (1987).
[32]L. V. Asryan, Quantum Electron. **35**, 1117 (2005).
[33]J. Hader, J. Moloney, and S. Koch, Appl. Phys. Lett. **99**, 181127 (2011).

[34]L. Bellaiche, T. Mattila, L.-W. Wang, S.-H. Wei, and A. Zunger, Appl. Phys. Lett. **74**, 1842 (1999).
[35]A. Reznitsky, A. Klochikhin, S. Permogorov, L. Tenishev, W. Lundin, A. Usikov, M. Schmidt, and C. Klingshirn, Phys. Status Solidi C **0**, 280 (2003).
[36]A. Levanyuk and V. Osipov, Phys. Usp. **24**, 187 (1981).
[37]E. O. Kane, J. Phys. Chem. Solids **1**, 249 (1957).
[38]M. Jacobson, D. Nelson, O. Konstantinov, and A. Matveentsev, Semiconductors **39**, 1410 (2005).
[39]A. Nirschl, M. Binder, M. Schmid, I. Pietzonka, H.-J. Lugauer, R. Zeisel, M. Sabathil, D. Bougeard, and B. Galler, Opt. Express **24**, 2971 (2016).
[40]K. W. Williams, N. R. Monahan, D. D. Koleske, M. H. Crawford, and X.-Y. Zhu, Appl. Phys. Lett. **108**, 141105 (2016).
[41]S. Y. Karpov, Proc. SPIE **9768**, 97680C (2016).
[42]E. Rashba and G. Gurgenishvili, Phys. Solid State **4**, 759 (1962).
[43]J. Feldmann, G. Peter, E. O. Göbel, P. Dawson, K. Moore, C. Foxon, and R. J. Elliott, Phys. Rev. Lett. **59**, 2337 (1987).
[44]A. V. Kavokin, Phys. Rev. B **50**, 8000 (1994).
[45]G. Callsen, G. M. O. Pahn, S. Kalinowski, C. Kindel, J. Settke, J. Brunnmeier, C. Nenstiel, T. Kure, F. Nippert, A. Schliwa, A. Hoffmann, T. Markurt, T. Schulz, M. Albrecht, S. Kako, M. Arita, and Y. Arakawa, Phys. Rev. B **92**, 235439 (2015).